

Markov-Parameter-Based Adaptive Control of 3-Axis Angular Velocity in a Six-Degree-of-Freedom Stewart Platform

Benjamin L. Pence[†], Mario A. Santillo[‡], and Dennis S. Bernstein[‡]

[†]Department of Mechanical Engineering
University of Michigan
Ann Arbor, MI 48109
{bpence}@umich.edu

[‡]Department of Aerospace Engineering
University of Michigan
Ann Arbor, MI 48109
{santillo, dsbaero}@umich.edu

Abstract—Stewart platforms are complex mechanical devices used throughout industry for vibration testing and precision pointing applications. These platforms are nonlinear, strongly coupled MIMO systems. For a six-degree-of-freedom Stewart platform, we consider the problem of three-degree-of-freedom angular-velocity command following. Static nonlinearity inherent in the platform is analyzed, and a closed-loop setup for adaptive command-following control is described. A review of the Markov-parameter-based adaptive control algorithm is given, along with the OKID system identification algorithm, test procedures, and experimental results.

I. INTRODUCTION

A Stewart platform is a device for producing multi-degree-of-freedom motion. These devices are widely used in the entertainment industry, for aircraft simulation, and for testing the performance and robustness of a wide range of products in a high-vibration environment [1–3]. Stewart platforms are available in various realizations; key differentiators include translational versus rotational actuators, as well as hydraulic versus electric actuation. These devices range in size from a few centimeters in size to many meters, with payloads ranging from below a kilogram to many tons [4–7].

Precision control of a Stewart platform is challenging due to the kinematic nonlinearity of the device, the dynamics of the motors and amplifiers, and the fact that the system is multivariable and highly coupled. An additional complicating factor concerns the type of measurement signals that are available, namely, displacement, velocity, or acceleration, as well as their location on the platform, for example, colocated with the actuators or with the payload [8].

Control of Stewart-platform motion typically involves real-time solution of the inverse kinematics. This approach is computationally intensive and requires an accurate model that can be linearized [9–11]. In the present work we adopt an adaptive control approach in which we use measurements to improve the dynamic performance of the system through on-line tuning. In particular, we consider the experimental application of an adaptive control algorithm to a six-degree-

of-freedom Stewart platform in the Vibration, Acoustics, and Motion Control Laboratory at the University of Michigan, as shown in Figure 1.

To do this, we first assess the static nonlinearity present in the system by commanding the platform at low frequency and by using a six-degree-of-freedom displacement sensor to measure command-following errors. No analytical or CAD model of the platform geometry is used or is assumed to be available in this work. We next focus our attention on adaptive control for dynamic performance. For this objective, we use a 3-axis angular velocity sensor for feedback and use command-following angular-velocity errors as the feedback signal.

For adaptive control under dynamic conditions, we use the Markov-parameter-based adaptive control algorithm developed in [12, 13]. This adaptive control algorithm requires knowledge of only the first nonzero Markov parameter. Since the algorithm is fully digital, no discretization is required, and the algorithm can be implemented directly. The observer/Kalman filter identification (OKID) algorithm [14] is used to estimate a bound on the first nonzero Markov parameter. The adaptive algorithm of [12, 13] assumes that the plant is minimum phase, an assumption that we do not attempt to verify for the Stewart platform. The variant of [12, 13] given in [15] is known to be effective for nonminimum phase systems, but is more computationally intensive.

II. STEWART PLATFORM

The experimental facility, located in the Vibration, Acoustics, and Motion Control Laboratory at the University of Michigan, is a six-degree-of-freedom Stewart platform (see Figure 1). This platform consists of a 3-foot-square aluminum table with threaded holes on a 2-inch-square grid, supported by six rigid struts, each of which is connected to the casing of an electric motor. The platform is capable of motion in six degrees of freedom, that is, surge, heave, sway, yaw, pitch, and roll. The platform has the ability to

move in any single axis or any combination of axes. A BEI Motionpak triaxial accelerometer and gyro sensor is mounted on the table to measure translational acceleration and angular velocity [16].

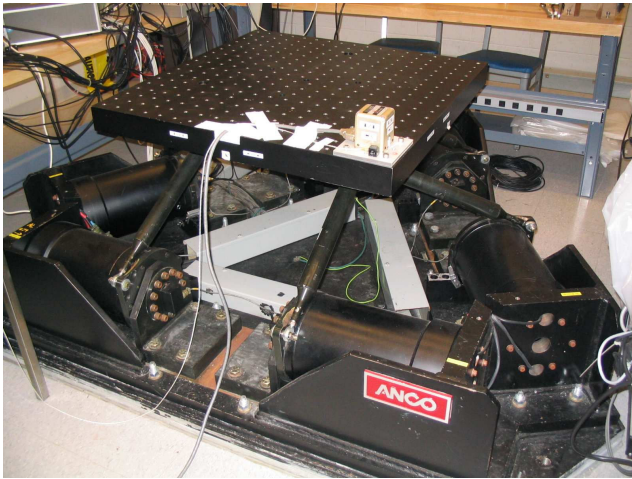


Fig. 1. Six-degree-of-freedom Stewart platform.

The platform is capable of translational displacement up to ± 2.5 inches in each axis, and angular displacement up to ± 5 deg in each axis, with acceleration levels up to 9 g with minimal payload. The frequency response is up to 130 Hz. The platform carries a payload capacity of 400 lb and is force rated up to 1440 lb. The platform is actuated by six electric motors, each driven by a controller and amplifier. Each motor is capable of 370 ft-lb torque, with a peak power requirement of 6 kW at 200 VAC, 3-phase power. The amplifiers and controllers, which are commanded by software, operate in torque-commanded mode, using digital encoder feedback from the six motors. A mixer box is used to convert between user commands and motor torque commands. The mixer box also contains a linear inverse kinematics model of the motor/linkage geometry, so as to approximately decouple the commands and achieve an approximately diagonal transfer-function matrix.

Communication and control are achieved by means of a dSPACE 1103 processor connected to a Microsoft Windows-based PC. Controllers are programmed using Matlab and Simulink, compiled by Real-Time Workshop, and loaded onto the dSPACE 1103 for closed-loop operation. Communication is handled through a terminal board connected to the PC, which has both analog and digital inputs and outputs. The terminal board is directly connected to the platform's sensors and actuators. The dSPACE 1103 is capable of storing either one channel of data sampled at 512 Hz for approximately 2 minutes, or 20 sec of data with all six channels in use.

Translation and displacement of the platform is measured by means of a Polhemus Liberty sensor system [17]. This system uses RF-modulated magnetic signals to determine displacement in six degrees of freedom. The system, which

uses a receiver and sensor that are noncontacting, can measure displacement over the full range of motion of the platform. The accuracy of these measurements is below 0.1 inch and 0.1 deg, while the resolution and repeatability are approximately an order of magnitude better. The sample rate for all 6 signals is 240 Hz, and data are obtained through the RS232 interface of the dSPACE 1103 system. In the present paper, the Polhemus sensor is used for the static performance assessment.

The triaxial accelerometer is capable of measuring accelerations up to 10 g, while the triaxial gyro is capable of measuring angular velocities up to 500 deg/sec. Since angular displacements are small, we assume that all rotations commute, which simplifies the interpretation of angular velocity data. In the present paper, the triaxial gyro is used for feedback and dynamic performance assessment.

The platform is programmed with inner PID loops to provide stiffness, damping, and zero steady-state error for step commands, see Figure 2. These loops, which use resolver-synthesized encoder signals, stabilize the platform to a unique displacement and make it possible to close angular rate loops with angular rate performance variables. Without an asymptotically stable equilibrium, the platform would drift under angular rate control.

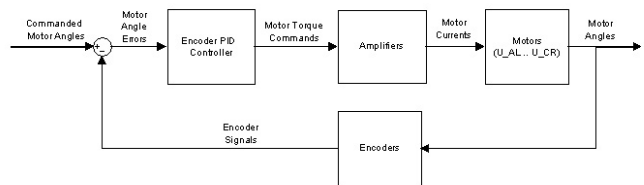


Fig. 2. Platform inner PID loops, which provide stiffness, damping, and zero steady-state error for step commands.

III. STATIC PERFORMANCE ASSESSMENT

Our first consideration is to assess the static kinematic nonlinearity of the platform. Nonlinearity arises from the motor/linkage geometry in the presence of the mixer-box inverse kinematics. To quantify the static nonlinearity, we use an input displacement-command sequence consisting of low-frequency content for each of the six input channels. This input command is implemented on the platform, and output measurements are sampled at 512 Hz. A comparison plot of displacement command and output response is shown in Figure 4 for all six channels. The division between command and output suggests that static nonlinearity is inherent in the platform. The RMS error between command and output response is 0.015 in, 0.013 in, 0.016 in, 0.044 deg, 0.039 deg, 0.017 deg for the x , y , z , R_x , R_y , and R_z channels, respectively. The x , y , and z channels represent linear displacements, while the R_x , R_y , and R_z channels represent angular displacements around the X , Y , and Z axes, respectively.

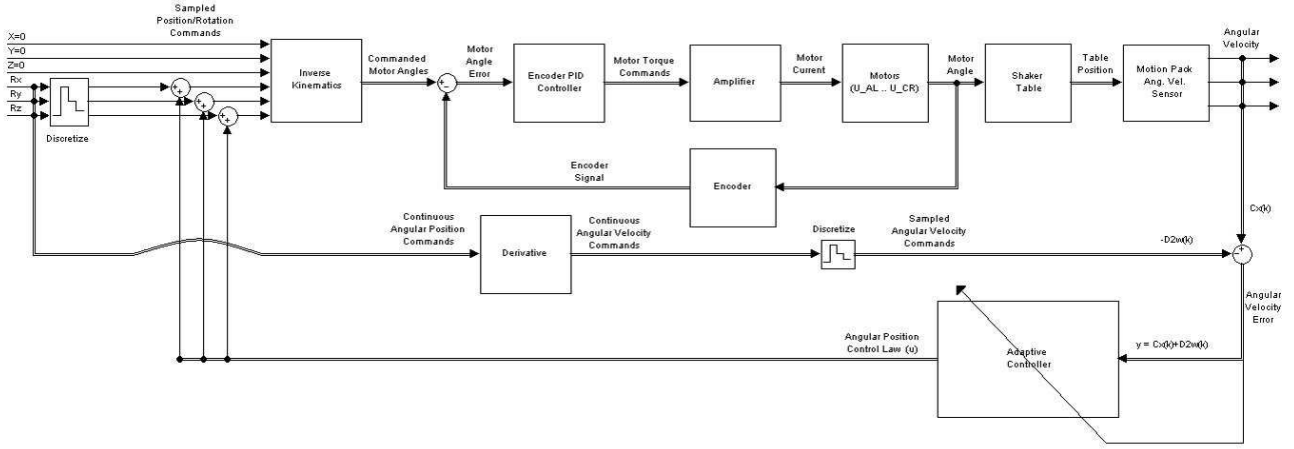


Fig. 3. Block diagram of the closed-loop adaptive control architecture for the six-degree-of-freedom Stewart platform.

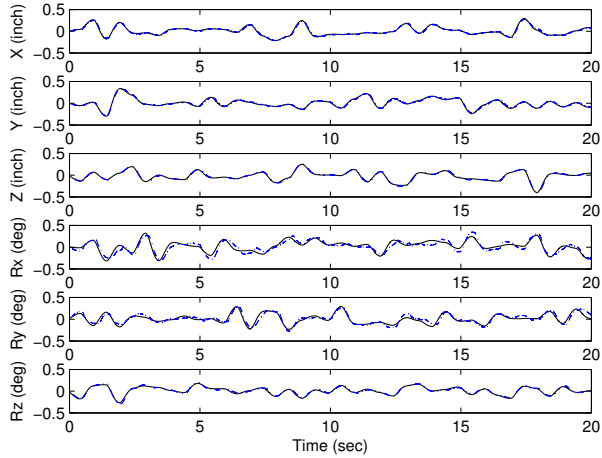


Fig. 4. Comparison of displacement command (solid) and output response (dashed) for all six channels using the Polhemus sensor. The division between command and output suggests that static nonlinearity is inherent in the Stewart platform.

These results quantify the kinematic nonlinearity in the platform. This kinematic nonlinearity can be compensated for by means of nonlinear inversion or by iterated learning control [18] using position measurements. However, we now focus our attention on the dynamic performance of the platform, namely, the ability of the platform to follow angular velocity commands.

IV. DYNAMIC PERFORMANCE ASSESSMENT

The block diagram in Figure 3 depicts the closed-loop adaptive control architecture for the platform. We consider only triaxial angular displacement commands and triaxial angular velocity measurements, thus constituting a 3-input, 3-output dynamic subsystem. Translational position commands are set to zero, and the accelerometer measurements are not recorded. The platform is open-loop commanded

using an angular displacement command that is represented analytically as a continuous-time signal. The displacement commands are then discretized and input to the platform. Since the angular displacement commands are represented analytically, the corresponding continuous-time derivatives are available. These derivatives can be viewed as angular velocity commands, which are compared to the angular velocity measurements \dot{R}_x , \dot{R}_y , and \dot{R}_z to provide rate errors. The objective is to reduce the performance variable to zero, that is, follow angular velocity commands by closed-loop adaptive control using triaxial angular velocity measurements.

We assess dynamic performance using single-frequency sinusoids in each axis, as seen in Figure 5. This figure shows open-loop angular-velocity errors for tonal angular-displacement commands at 20 Hz, 21 Hz, and 22 Hz with amplitudes of 0.05 deg about the X , Y , and Z axes, respectively. The corresponding angular-velocity commands have frequencies of 20 Hz, 21 Hz, and 22 Hz with amplitudes of 6.28 deg/sec, 6.60 deg/sec, and 6.91 deg/sec about the X , Y , and Z axes, respectively. These amplitudes are of the same order as the open-loop angular-velocity command-following errors shown in Figure 5.

V. ADAPTIVE ALGORITHM

We now provide a brief overview of the key components of the Markov-parameter-based adaptive control algorithm given in [13]. Consider the multi-input multi-output (MIMO) discrete-time system

$$x(k+1) = Ax(k) + Bu(k) + D_1w(k), \quad (1)$$

$$y(k) = Cx(k) + D_2w(k), \quad (2)$$

where $x(k) \in \mathbb{R}^n$, $y(k) \in \mathbb{R}^l$, $u(k) \in \mathbb{R}^l$, $w(k) \in \mathbb{R}^{l_w}$, and $k \geq 0$. Our goal is to design an adaptive output feedback controller under which the performance variable y converges to zero in the presence of the exogenous signal w . Note that

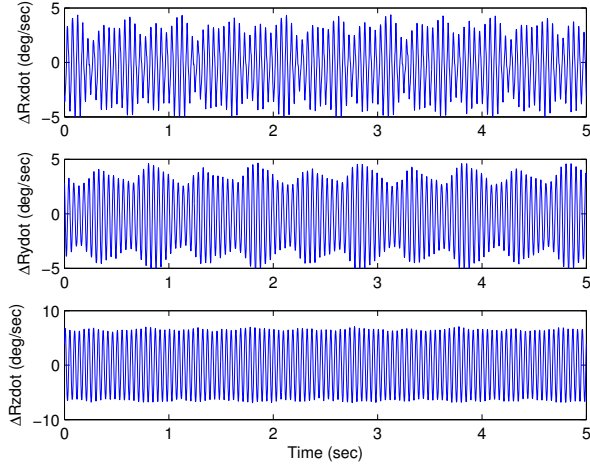


Fig. 5. Open-loop angular-velocity command-following errors for tonal angular displacement commands at 20 Hz, 21 Hz, and 22 Hz with amplitudes of 0.05 deg about the X, Y, and Z axes, respectively, or equivalently, tonal angular velocity commands at 20 Hz, 21 Hz, and 22 Hz with amplitudes of 6.28 deg/sec, 6.60 deg/sec, and 6.91 deg/sec about the X, Y, and Z axes, respectively. The open-loop angular-velocity command-following errors are of the same order as the angular velocity commands.

w can represent either a command signal to be followed, an external disturbance to be rejected, or both.

Next, define the transfer function matrix

$$G_{yu}(z) \triangleq C(zI - A)^{-1}B = \sum_{i=d}^{\infty} z^{-i}H_i, \quad (3)$$

and define d to be the smallest positive integer i such that the i th Markov parameter $H_i \triangleq CA^{i-1}B$ is nonzero. We make the following assumptions:

- (A1) The triple (A, B, C) is controllable and observable.
- (A2) If $\lambda \in \mathbb{C}$ and $\text{rank} \begin{bmatrix} A - \lambda I & B \\ C & 0 \end{bmatrix} < \text{normal rank} \begin{bmatrix} A - zI & B \\ C & 0 \end{bmatrix}$, then $|\lambda| < 1$.
- (A3) d is known.
- (A4) H_d is nonsingular.
- (A5) There exists $\bar{H}_d \in \mathbb{R}^{l \times l}$ such that $2H_d^T H_d \leq H_d^T \bar{H}_d + \bar{H}_d^T H_d$ and \bar{H}_d is known.
- (A6) There exists an integer \bar{n} such that $n \leq \bar{n}$ and \bar{n} is known.
- (A7) The performance variable $y(k)$ is measured and available for feedback.
- (A8) The exogenous signal $w(k)$ is generated by

$$x_w(k+1) = A_w x_w(k), \quad (4)$$

$$w(k) = C_w x_w(k), \quad (5)$$

where $x_w \in \mathbb{R}^{n_w}$ and A_w has distinct eigenvalues, all of which are on the unit circle.

- (A9) There exists an integer \bar{n}_w such that $n_w \leq \bar{n}_w$ and \bar{n}_w is known.
- (A10) The exogenous signal $w(k)$ is not measured.

(A11) $A, B, C, D_1, D_2, A_w, C_w, n, n_w$, and H_d are not known.

Next, consider the time-series controller

$$u(k) = \sum_{i=1}^{n_c} M_i(k)u(k-i) + \sum_{i=1}^{n_c} N_i(k)y(k-i), \quad (6)$$

where,

$$n_c \geq (l+1)\bar{n} + 2l\bar{n}_w - d, \quad (7)$$

and, for all $i = 1, \dots, n_c$, $M_i : \mathbb{N} \rightarrow \mathbb{R}^{l \times l}$ and $N_i : \mathbb{N} \rightarrow \mathbb{R}^{l \times l}$ are given by the adaptive law presented below. The control can be expressed as

$$u(k) = \theta(k)\phi(k), \quad (8)$$

where

$$\theta(k) \triangleq \begin{bmatrix} N_1(k) & \cdots & N_{n_c}(k) & M_1(k) & \cdots & M_{n_c}(k) \end{bmatrix} \quad (9)$$

and

$$\phi(k) \triangleq \begin{bmatrix} y(k-1) \\ \vdots \\ y(k-n_c) \\ u(k-1) \\ \vdots \\ u(k-n_c) \end{bmatrix}. \quad (10)$$

We define the cost function

$$\mathcal{J}(k) \triangleq \frac{1}{2}y^T(k)y(k), \quad (11)$$

and define $\tilde{\theta}(k) \triangleq \theta(k) - \theta_*$, where θ_* is the ideal controller parameter, which, for all $k \geq k_0$, yields $y(k) = H_d \tilde{\theta}(k-d)\phi(k-d)$. The time step k_0 is given by $k_0 \triangleq n_o + n_c + d - m$, where $n_o \leq lm$ and $m \leq n$. The gradient of $\mathcal{J}(k)$ with respect to $\tilde{\theta}(k-d)$ is given by

$$\frac{\partial \mathcal{J}(k)}{\partial \tilde{\theta}(k-d)} = H_d^T y(k)\phi^T(k-d). \quad (12)$$

Since, by assumption (A11), H_d is unknown, we replace H_d in (12) with \bar{H}_d , and, in place of (12), we use the implementable gradient

$$G(k) \triangleq \bar{H}_d^T y(k)\phi^T(k-d). \quad (13)$$

Note that the implementable gradient (13) can be used in practice due to assumptions (A3), (A5), and (A7).

Finally, the update law for the controller parameter $\theta(k)$ is given by

$$\theta(k+1) = \theta(k-d) - \eta(k)G(k), \quad (14)$$

where $\eta : \mathbb{N} \rightarrow [0, \infty)$ is a step-size function. Note that if $G(k) = 0$ then $\eta(k)$ is irrelevant. In accordance with assumptions (A10) and (A11), the adaptive control law (14) does not require a measurement of the exogenous signal $w(k)$

and does not use knowledge of the exogenous dynamics (4), (5).

Furthermore, for all $k \geq k_0$, let $\zeta(k) \in \mathbb{R}$ be such that

$$0 < \inf_{j \geq k_0} \zeta(j) \leq \zeta(k) \leq \sup_{j \geq k_0} \zeta(j) < 2, \quad (15)$$

and, for all $k \in \mathbb{N}$ such that $G(k) \neq 0$, let $\eta(k) \in [0, \infty)$ satisfy

$$\eta(k) = 0, \quad \text{if } k < k_0, \quad (16)$$

$$\eta(k) = \zeta(k)\eta_{\text{opt}}(k), \quad \text{if } k \geq k_0, \quad (17)$$

where

$$\eta_{\text{opt}}(k) \triangleq \frac{\|y(k)\|_2^2}{\|G(k)\|_F^2}. \quad (18)$$

Then, for all initial conditions $x(0)$ and $\theta(0)$, $\theta(k)$ is bounded, $u(k)$ is bounded, $\lim_{k \rightarrow \infty} y(k) = 0$, and $x(k)$ satisfying (1) is bounded. A closed-loop stability proof is given in [13].

VI. MARKOV-PARAMETER ESTIMATION

To estimate the required controller parameters for the Markov-parameter-based adaptive control algorithm, an open-loop identification experiment is conducted using band-limited white noise signals to command simultaneous angular displacement motion in all three axes, while triaxial angular velocity sensor measurements are recorded at a sampling rate of 512 Hz. Translational commands are set to zero throughout the identification experiment. This setup constitutes a 3-input, 3-output subsystem from angular displacement commands to angular velocity measurements, and hence $l = 3$.

Data from the open-loop experiment are used with the OKID algorithm [14] to estimate the Markov parameters of the plant (A, B, C) . This algorithm requires no prior statistical information and does not rely on sample correlation or covariance calculations. The OKID algorithm acts as an optimal observer in the presence of noise [14].

Figure 6 shows the first 50 Markov parameters obtained from OKID, from commanded triaxial angular displacements to measured triaxial angular velocities. Each Markov parameter has 9 scalar entries corresponding to the transfer function from the angular displacement command to the measured angular velocity. From Figure 7, and using engineering judgment, the relative degree is taken to be $d = 7$. Therefore, the bound \bar{H}_7 on the first nonzero Markov parameter is chosen to be

$$\bar{H}_7 = \begin{bmatrix} -0.2 & 0 & 0 \\ 0 & 0.2 & 0 \\ 0 & 0 & -0.4 \end{bmatrix}. \quad (19)$$

This matrix is used in the following section to conduct a closed-loop adaptive command-following experiment.

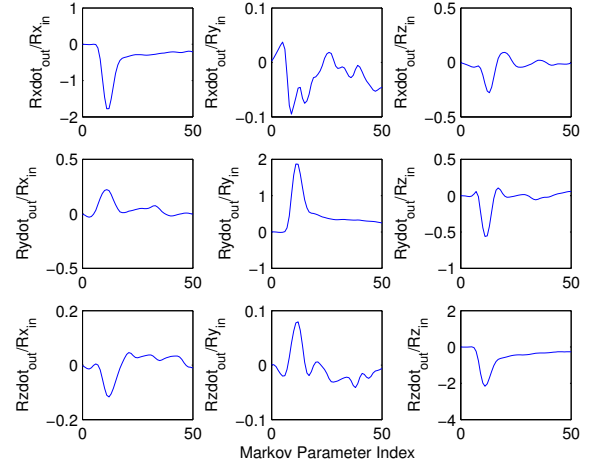


Fig. 6. All 9 entries of the first 50 Markov parameters from commanded triaxial angular displacement to measured triaxial angular velocity. Each curve represents 50 data points.

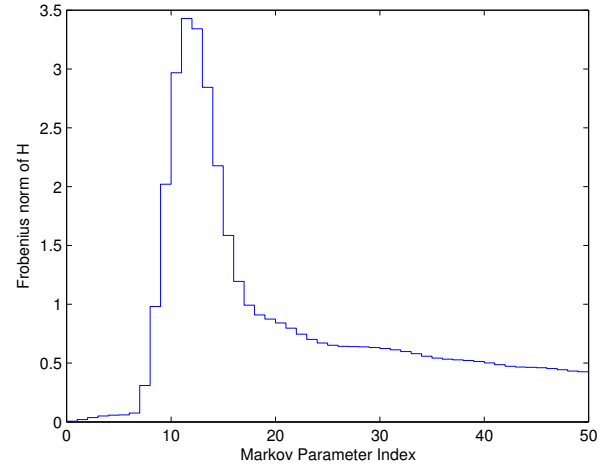


Fig. 7. Frobenius norm of the first 50 Markov parameter estimates. The step from \bar{H}_6 to \bar{H}_7 suggests that the relative degree d of the system is 7.

VII. ADAPTIVE CONTROL EXPERIMENT

The objective of the experiment is to follow angular velocity commands by closed-loop adaptive control using triaxial angular velocity sensor measurements. The experiment injects tonal signals as angular displacement commands. The command frequencies are chosen to be 20 Hz, 21 Hz, and 22 Hz, respectively, about the X, Y, and Z axes. The amplitude of the angular displacement command is 0.05 deg in all three axes. The corresponding angular-velocity commands have frequencies of 20 Hz, 21 Hz, and 22 Hz with amplitudes of 6.28 deg/sec, 6.60 deg/sec, and 6.91 deg/sec about the X, Y, and Z axes, respectively. The 3×3 MIMO adaptive controller order is chosen to be $n_c = 35$ and $\zeta(k) \equiv 1/4555555$ is used. Commands and measurements are sampled at a rate of 512 Hz.

The platform is run in closed-loop for approximately 10 min. A plot comparing open-loop and closed-loop angular-velocity errors is provided in Figure 8. Here, open-loop triaxial angular-velocity errors for a period of 20 seconds are seen on the left-hand side, while closed-loop triaxial angular-velocity errors for the last 20 seconds of the experiment are seen on the right-hand side. Values of $\zeta(k)$ larger than $1/100000$ generally cause the controller to adapt too quickly, inciting unacceptable transients.

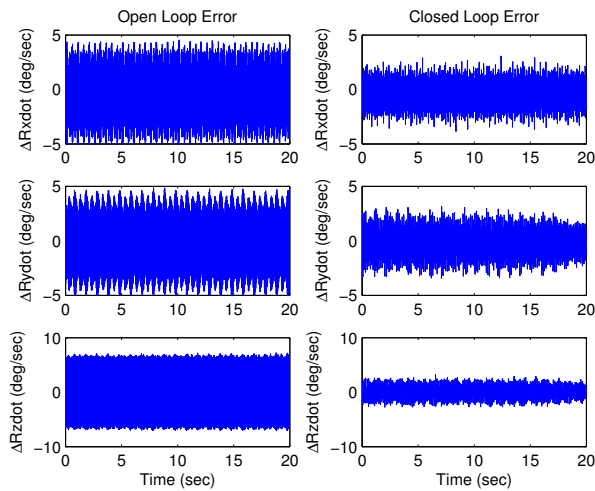


Fig. 8. Open-loop and closed-loop performance angular-velocity errors for tonal angular-displacement commands at 20 Hz, 21 Hz, and 22 Hz with amplitudes of 0.05 deg. The left-hand-side shows open-loop angular-velocity errors for a period of 20 seconds, while the right-hand-side shows closed-loop angular-velocity errors for the last 20 seconds of the experiment. The RMS error is reduced by at least a factor of 2 in all axes.

Using the data from Figure 8, RMS angular-velocity errors are calculated for each axis. From open-loop to closed-loop, both X - and Y -axis RMS errors are reduced by a factor of 2, while the Z -axis RMS error is reduced by a factor of 4.

VIII. CONCLUSIONS

We conducted a MIMO closed-loop adaptive command-following experiment using a six-degree-of-freedom Stewart platform. An overview of the experimental facility located at the University of Michigan was given. Static nonlinearity inherent in the platform was analyzed and a closed-loop setup to conduct adaptive command-following experiments was described. A review of the Markov-parameter-based adaptive control algorithm was given, along with a system identification algorithm, test procedures, and experimental results. Closed-loop experiments were shown to reduce RMS angular-velocity errors by at least a factor of 2 in all axes during a 10 minute test. Future work includes extending this experiment to the 6-input, 6-output case.

REFERENCES

- [1] F. Jafari and J. E. McInroy, "Transfer matrices of orthogonal Gough-Stewart platforms," in *Proc. Conf. Dec. Contr.*, Maui, HI, 2003, pp. 5865–5870.
- [2] J. E. McInroy and S. S. Aphale, "Optimal filters from task velocities to joint velocities including both position and velocity limits," in *Proc. Conf. Dec. Contr.*, Maui, HI, 2003, pp. 5885–5890.
- [3] P. Renaud, N. Andreff, G. Gogu, and P. Martinet, "On vision-based kinematic calibration of n-leg parallel mechanisms," in *13th IFAC Symposium on Sys. Id.*, Rotterdam, the Netherlands, August 2003, pp. 977–982.
- [4] "Moog FCS control systems," Moog FCS Inc., September 2007, <http://www.moog-fcs.com/>.
- [5] "Design & manufacturing engineering, robotics," Pacific Northwest Laboratory, September 2007, <http://www.technet.pnl.gov/dme/>.
- [6] "Precision 6-axis stages, robotics, parallel kinematics, nanopositioning, micropositioning," Physik Instrumente (PI) GmbH & Co. KG, September 2007, <http://www.hexapods.net/>.
- [7] "Hexapods," SYMETRIE, September 2007, <http://www.symetrie.fr/>.
- [8] J. Chandrasekar and D. S. Bernstein, "Position control of a two-bar linkage with acceleration-based identification and feedback," in *Proc. Amer. Contr. Conf.*, Portland, OR, 2005, pp. 1987–1992.
- [9] P. Nana, K. J. Waldron, and V. Murthy, "Direct kinematic solution of a Stewart platform," *IEEE Trans. Robot. Autom.*, vol. 6, pp. 438–444, 1990.
- [10] R. S. Stoughton and T. Arai, "A modified Stewart platform manipulator with improved dexterity," *IEEE Trans. Robot. Autom.*, vol. 9, pp. 166–173, 1993.
- [11] B. Dasgupta and T. S. Mruthunjaya, "The Stewart platform manipulator: a review," *Mech. and Mach. Thy.*, vol. 35, pp. 15–40, 2000.
- [12] J. B. Hoagg and D. S. Bernstein, "Adaptive stabilization, command following, and disturbance rejection for minimum phase discrete-time systems," in *Proc. Conf. Dec. Contr.*, San Diego, CA, 2006, pp. 471–476.
- [13] J. B. Hoagg, M. A. Santillo, and D. S. Bernstein, "Discrete-time adaptive command following and disturbance rejection with unknown exogenous dynamics," *IEEE Trans. Autom. Contr.*, (to appear).
- [14] J. N. Juang, *Applied System Identification*. Upper Saddle River, NJ: Prentice-Hall, 1993.
- [15] R. Venugopal and D. S. Bernstein, "Adaptive disturbance rejection using ARMA/Toeplitz models," *IEEE Trans. Contr. Sys. Tech.*, vol. 8, pp. 257–269, 2000.
- [16] "BEI Motionpak multi-axis inertial sensing system," BEI Technologies, Inc., September 2007, <http://www.polhemus.com/>.
- [17] "Polhemus LIBERTY electromagnetic motion tracking system," Polhemus, September 2007, <http://www.systron.com/>.
- [18] D. A. Bristow, M. Tharayil, and A. G. Alleyne, "A survey of iterative learning control," *IEEE Contr. Sys. Mag.*, vol. 26, pp. 96–114, 2006.